A new design technique based on a suitable choice of rotor geometrical parameters to maximize torque and power factor in synchronous reluctance motors: Part II - Finite-element analysis and measurements

Ivan Eduardo Chabu   Viviane Cristine Silva
José Roberto Cardoso   Silvio I. Nabeta
LMAG/ EPUSP - Escola Politécnica da Universidade de São Paulo
Av. Prof. Luciano Gualberto, Trav. 3, 158 - 05508-900 São Paulo SP - Brazil

Albert Foggia
LEG - Laboratoire d'Electrotechnique de
Grenoble - BP 46 - F-38402
St. Martin d'Hères Cedex - France

Abstract - The influence of rotor geometry of synchronous reluctance motors (SRMs) on the x_d/x_q ratio, electromagnetic torque and iron losses is studied. Both air-gap length and rotor pole arc are taken into account as parameters. In a companion paper (Part I-Theory) a new theoretical approach was developed neglecting saturation effects. Here (Part II), the analytical determination of the parameters and the machine behaviour is performed for a particular SRM, on the statement of Part I, including saturation effects. Also a complete finite-element analysis is carried out, followed by a comparison with results obtained by tests performed in a prototype machine, which was constructed in order to validate the proposed methodology.

Keywords: Synchronous Reluctance Machines, synchronous machine design, reluctance motors.

I. INTRODUCTION

In a companion paper (Part I-Theory) [1], a theoretical analysis was proposed which gives some guidance so as to optimize rotor geometry of synchronous reluctance motors (SRM) with the aim of maximizing both torque and power factor keeping the iron losses in satisfactory limits. It also permits to analyse mechanical constraints, such as the adequate placements of the starting cage.

Althought that analysis is linear, many conclusions arise from the equations and curves that are functions of the x_d/x_q ratio.

Thus, concerning the saturation effects, it seems to be sufficiently accurate to work with saturated values of this ratio, x_d/x_q, in the related equations. It is important to note that the saturation levels of the magnetic circuit are different for the direct and quadrature axes, specially in the voltage-source mode operation. So, the calculation method may consider distinct saturation factors for evaluating x_d and x_q.

In this paper, the proposed methodology will be applied in a prototype machine; a 4-pole, 380 V, 60 Hz, 11.2 KW, used in a constant voltage mode. The cross section of its magnetic circuit is presented in Fig.1.
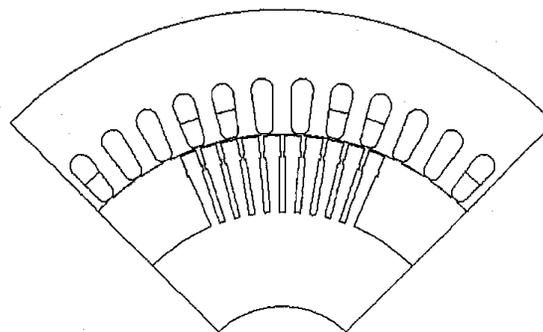

Fig.1. Machine cross section-one pole

The rotor construction is simpler, when compared to other possible geometries, which allows a reduction in the manufacturing cost.

Appendix I presents the dimensions and the construction data for the SRM.

The relatively large number of long narrowed rotor teeth are used as a way to let them into a strong saturation level in the quadrature axis. It leads to a reduction in the quadrature reactance and consequently to a improvement in the x_d/x_q ratio.

In this work, the calculation will be performed by analytical methods as well as by numerical simulations using a 2D-Finite element package.

The results will be compared to experimental data.

II. ANALYTICAL CALCULATIONS

The main objectives of this section is to evaluate the reactances x_d and x_q allowing for the saturated magnetic circuit in both axes.

The procedure is similar to that usually applied to classical machines [3]. The effective phase-winding submitted to the rated voltage and frequency generates a flux per pole which determines the flux density and the magnetomotive force (mmf) in each part of the machine.

The total mmf required in each axis determines the magnetizing current, I_d and I_q, and consequently the saturated reactances x_d and x_q are obtained.

An important distinction may be considered at this point in order to calculate the flux density and the mmf of the air-gap and adjacent magnetic surfaces (stator and rotor teeth).

Differently from a machine with smooth air-gap, the SRM presents a flux density spatial distribution far from the sinusoidal shape. Thus, the shape factor of such distribution is a function of geometric parameters and may be evaluated independently for the air-gap, stator and rotor teeth, for both D and Q-axes.

Table I presents the shape factors using the results obtained in [1]:

Table I Shape factors

	Direct axis	Quadrature axis
Air-gap and stator teeth	$K_{FDS} = \dfrac{2}{\pi} \cdot f_D(\alpha, k)$	$K_{FQS} = \dfrac{2}{\pi} \cdot f_Q(\alpha, k)$
Rotor teeth	$K_{FDR} = \dfrac{2}{\alpha\pi} \cdot f_D(\alpha, k)$	$K_{FQR} = \dfrac{2}{\alpha\pi} \cdot f_Q(\alpha, k)$

where:

$$f_D(\alpha, k) = \left[k + (1-k)\sin\frac{\alpha\pi}{2} \right]$$

$$f_Q(\alpha, k) = \left[k + (1-k)\cos\frac{\alpha\pi}{2} \right]$$

Another important fact to be taken into account in the calculation is the correct consideration of the air-gap flux weakening due to stator leakage reactance, x_a, when the rotor passes from the D-axis to the Q-axis. This evaluation may be performed by an iterative computation of the currents I_d and I_q or by means of a graphical solution of the magnetic circuit.

Fig. 2 shows the two magnetizing characteristics of the SRM, computed for the D and Q axes.

In Fig.2, the points A and B are the rated conditions of the magnetic circuit operating in constant voltage mode for the D and Q axes, respectively. The magnetizing component of the reactances are obtained from:

$$x_{dd} = \frac{V_A}{Id} \qquad x_{qq} = \frac{V_B}{Iq} \qquad (\Omega/\text{phase})$$

and the total reactances are:

$$x_d = x_{dd} + x_a = \frac{V_N}{I_d}; \qquad x_q = x_{qq} + x_a = \frac{V_N}{I_q} \qquad (\Omega/\text{phase})$$

Once the reactances are obtained the determination of the input active and reactive powers as function of the load angle δ becomes a simple task.

In [1] the equations (1) and (2) were obtained neglecting the stator resistance. In this work, in order to correctly evaluate the mechanical power and the efficiency, the stator phase resistance was taken into account. Thus the input active and reactive powers result, respectively:

$$P_{in} = \frac{V^2}{\left(x_d + \frac{r_a^2}{x_q} \right)} \left[\frac{r_a}{x_q} + \frac{1}{2}\left(\frac{x_d}{x_q} - 1 \right)\sin 2\delta \right] \quad (\text{W / phase})$$

$$Q_{in} = \frac{V^2}{\left(x_d + \frac{r_a^2}{x_q} \right)} \left[\left(\frac{x_d}{x_q} - 1 \right)\sin^2\delta + 1 \right] \quad (\text{VAr / phase})$$
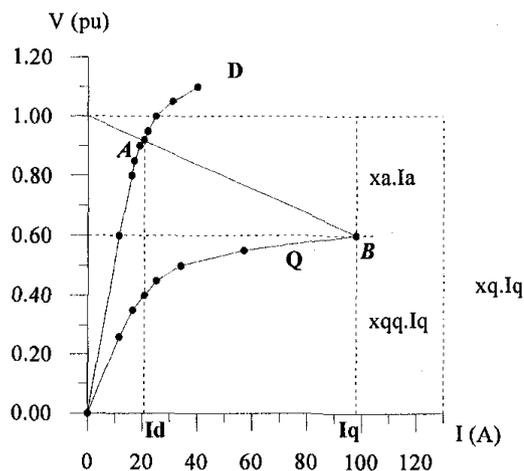

Fig.2. Magnetizing characteristics on D and Q axes

The resultant apparent power allows the evaluation of phase-current and also the Joule losses in stator winding.

The iron losses, P_{iron}, are evaluated by means of an usual method which considers an equivalent smooth rotor machine with the same rated flux. In this method the stator teeth component of the losses is multiplied by an increment factor, γ, as stated in [1].

The friction and windage losses as well as the stray load losses may also be computed.

The resultant mechanical power, P_{mech}, is obtained by subtracting the total losses from the total input power, allowing then the calculation of the efficiency and the power factor.

For the present case, using the construction data shown in Appendix I, we obtain:

D and Q axes air-gap ratio: $k = 1/68 = 0.0147$
Polar arc and pole pitch ratio: $\alpha = 0.52$
Shape factors obtained from Fig.8 of [1]:
    $k_{FDS} = 0.467 \quad k_{FQS} = 0.209$
    $k_{FDR} = 0.897 \quad k_{FQR} = 0.402$
Carter factor for the air-gap: 1.3
Basic flux per pole: $\phi_b = 0.0185$ Wb
Stator phase leakage reactance: $x_a = 0.80$ Ω/phase
Iron losses (for equivalent smooth air-gap): $P_{iron} = 902$ W
    stator teeth component: 350 W
    stator yoke component: 552 W
Friction and windings losses: 380 W

Following the procedures described in this section, the performance characteristics are obtained:

D axis reactance: x_d=10.7 Ω/phase
Q-axis reactance: x_q=2.24 Ω/phase
Maximum mechanical power: P_{max}=24.8 W
Power factor at rated mechanical power: p.f.=0.62
Efficiency at rated mechanical power: 86%

Obviously these values are subject to the precision in determining the reactances, and hence, to the solution of the magnetic circuit. Nevertheless the calculation procedure described is simple and fast when performed in a computational routine. Moreover the results have a good agreement with experimental results as presented further.

Fig.3. Flux distribution in D axis

III. FINITE ELEMENT ANALYSIS

The finite element analysis (FEA) is a well-established method to simulate electromagnetic devices, which enables local quantities such as flux density to be determined accurately, including saturation effects.

In this work, a 2D finite element package was employed to simulate the steady-state operation of the prototype machine.

The computations of the reactances x_d and x_q were carried out by two magnetostatic simulations.

As stated in Adkins [5] the determination of those reactances, mainly for x_q, by the relation of flux and current is not accurate for reluctance type machines due to the important presence of space harmonics of the flux density in the air-gap.

Another alternative to obtain those parameters is by means of the total energy.

Nevertheless, for high saturated machines the computation of the energy by the integral $E = \int H.dB$ considers the incremental permeability [6] that leads to small values of reactances which do not correspond to those assumed in the adopted theory.

To overcome these restrictions, the reactances were obtained by the relation of voltage and current.

The voltage, for each axis, was calculated by the expression:

$$V = 4.44.f.N.k_w.\phi_{max}$$

where: f: rated frequency
          N: number of turns per phase
          k_w: winding factor

The magnetostatics simulations provided the values of the maximum flux per pole, ϕ_{max}.

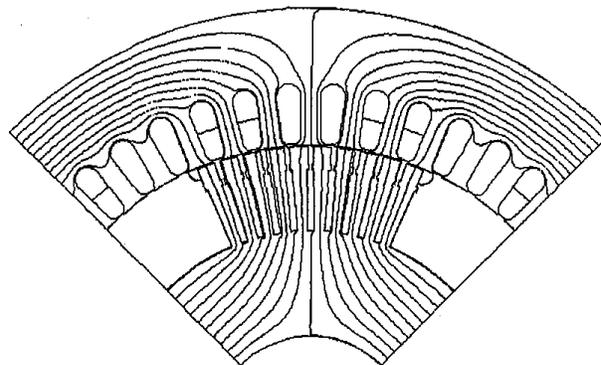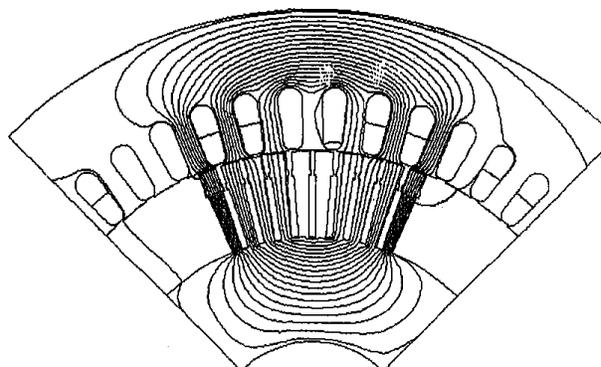Figures 3 and 4 show the flux distribution obtained for D and Q axes, respectively.

Fig.4. Flux distribution in Q axis

The FEA also allowed to compute the maximum torque, consequently the maximum output power, that occurs at δ=45°.

Fig.5 shows the flux distribution related to this analysis.

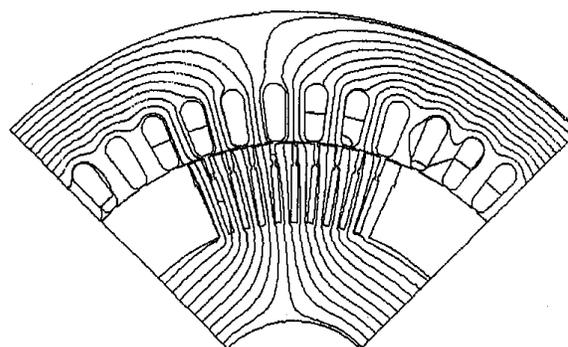Fig.5. Flux distribution for δ=45°

Results reached for x_d, x_q, and maximum output power, P_{max} are presented in the next section.

IV. EXPERIMENTAL RESULTS

The prototype SRM was submitted to tests in order to obtain the reactances and to measure the performance characteristics on load.

The D-axis reactance was measured by a simple no-load test at rated voltage while the Q-axis reactance was measured by a low-slip test under a voltage slightly lower than nominal.

The slow slip test is relatively difficult because the zero torque at Q-axis is unstable and the rotor is sustained in this condition by means of an external motor with sufficient power.

Although the external motor used was a DC machine in a Ward-Leonard scheme with good controlability, small fluctuations in the quadrature axis current could introduce some error in quadrature axis measurement.

The load test was performed in a DC dynamometer which yelded results with good accuracy.

The iron losses were roughly obtained by separating other losses so that parameter could be affected by an appreciable error.

Table II presents the comparison of x_d and x_q obtained by analytical and numerical methods.

By using those reactances of Table I, quantities such as the rated current, power factor and efficiency as well as the maximum output power were calculated and presented in Table III.

Table II: Reactances comparison

Parameter Method	x_d (Ω)	x_q (Ω)
Analytical	10.7	2.24
Numerical	9.8	2.42
Experimental	10.5	1.80

Table III: SRM quantities comparison

Parameter Method	I_n (A)	p.f.	η (%)	P_{max} (KW)
Analytical	32.2	0.62	86.0	24.8
Numerical	32.5	0.61	85.8	20.9*/21.5**
Experimental	35.8	0.56	84.8	23.3

* calculated through reactances   ** obtained directly from FEA

Fig. 6 shows the performance characteristics with load variation (angle δ) where one observes the good agreement between calculated and measured values.
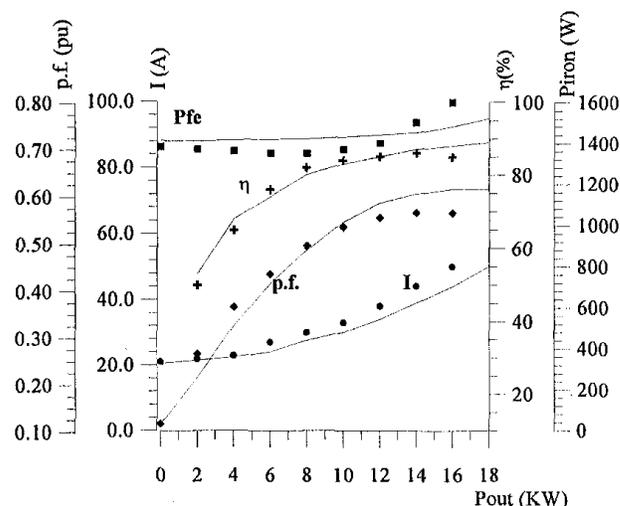

Fig.6. SRM characteristics with load variation
Analytical (solid lines) - Test (points)

V. CONCLUSIONS

New design procedures have been proposed in a companion paper, Part I of this work (Theory), so as to maximize both torque and power factor characteristics of SRMs. They are based on a theoretical analysis of the influence of rotor geometrical parameters (e.g. air-gap and pole arc) on those quantities. This influence, relating the electrical and mechanical quantities with geometrical parameters, is presented both in algebraic and graphical representation, thereby enabling the optimal choice of the relevant geometrical parameters.

This work corresponds to Part II, which presents a comparison between the previous methodology and measurements performed in a prototype SRM, as well as a numerical with the aid of a 2D finite element package.

The validation and efficiency of the analytical approach can be observed in the determination of global quantities when compared with the experimental data, as shown in Fig.6.

In the other hand, as long as local quantities are concerned it can be seen that the finite element analysis is more suitable than analytical procedures, especially when saturation effects are to be taken into account. It can be seen in Fig. 4 where the flux distribution and the evident high saturation of external teeth constitute a good starting point to optmize the ratio x_d/x_q by modifying the teeth width.

Finally, it has been shown that the proposed analytical method together with FEA provides an efficient and reliable tool for the design and optimization of SRMs.

VI. ACKNOWLEDGMENTS

and *USP-COFECUB* - Franco-brazilian cooperation program for the financial support during part of this work.

VII. APPENDIX I

SRM DIMENSIONAL DATA

pole-arc/pole-pitch ratio (α)	:	0.5
air-gap ratio (e_d/e_q)	:	1/69
stator internal diameter	:	210 mm
stator external diameter	:	310 mm.
motor lenght	:	230 mm
number of slots (stator)	:	48
tooth width (stator)	:	7.18 mm
number of slots per pole (rotor)	:	10
tooth width (rotor)	:	4.22 mm
air-gap in D-axis	:	0.45 mm
air-gap in Q-axis	:	30 mm
number of turns per phase	:	48
winding factor	:	0.925

VIII. REFERENCES

[1] I.E. Chabu, J.R. Cardoso, "Projeto de motores elétricos pelo método dos elementos finitos: comparação analítica/numérica/experimental", Proceedings of II SIMEAR - International Seminar in Electrical Machines and Drives, 07-09th. May 1991, São Paulo, pp. 83-99 (in Portuguese).

[2] I.E. Chabu, J.R. Cardoso, "A new design technique based on a suitable choice of rotor geometrical parameters to maximize torque and power factor in synchronous reluctance motors: Part I - Theory", Paper submitted to the IEEE International Electrical Machines and Drives Conference, Milwaukee, Wisconsin, May 18-21, 1997.

[3] M.G. Say, "Alternating current machines", Longman Scientific & Technical, 5th edition

[4] P.J. Lawrenson, L.A. Agu, "Theory and Performance of Polyphase Reluctance machines", Proc. IEE, vol. III, n° 8, Aug. 1964.

[5] B. Adkins, R.G. Harley, "The general theory of alternating current machines", Chapman and Hall, London, 1978.

[6] D.A. Lowther, P.P. Silvester, "Computer-aided design in magnetics", Springer Verlag, 1986.

IX. BIOGRAPHIES

Ivan Eduardo Chabu was born in São Paulo, Brazil, in June 3, 1955. He obtained the B.Sc. and M.Sc. degrees in Electrical Engineering from *Escola Politécnica da Universidade de São Paulo* (EPUSP), Brazil. At the present he is pursuing the Ph.D. degree at EPUSP. He is currently working as a Lecturer at EPUSP and in the industry in design and construction of electrical machines. His main research interests are design of special electric machines and electromagnetic devices.

Viviane Cristine Silva was born in São Paulo, Brazil, in November 27, 1962. She obtained the BSc and MSc degrees in Electrical Engineering from *Escola Politécnica da Universidade de São Paulo* (EPUSP), Brazil. In 1994 she obtained the PhD degree in Electrical Engineering from *Institut National Polytechnique de Grenoble* (INPG), France. She is currently working as a Researcher at LMAG/EPUSP on Modelling and CAD in Electromagnetics. Her main research interests are 2D and 3D FE computation on electromagnetic fields

Silvio Ikuyo Nabeta was born in São Paulo, Brazil, in July 2, 1960. He obtained the BSc and MSc degrees in Electrical Engineering from *Escola Politécnica da Universidade de São* Paulo (EPUSP), Brazil. In 1994 he obtained the PhD degree in Electrical Engineering from *Institut National Polytechnique de Grenoble* (INPG), France. He is currently working as a Lecturer at EPUSP and his main research interests are 2D FE modelling of electrical machines and numerical techniques

José Roberto Cardoso was born in 1949. He obtained the B.Sc., M.Sc., Ph.D. and Liv.Doc. from *Escola Politécnica da Universidade de São Paulo* (EPUSP), Brazil, in 1974, 1979, 1985 and 1993, respectively. In 1975 he joined the Dept. of Electrical Engineering, EPUSP, as an Assistant Professor. He was promoted to Doctor Professor and Associate Professor in 1985 and 1993, respectively. In 1988 he founded the *LMAG-Laboratório de Eletromagnetismo Aplicado*. He was an invited researcher in *LEG-Laboratoire d'Electrotechnique de Grenoble*, France, in 1987/88. His current research interest includes electromagnetic field computation by FEM and electrical machines. He is currently the COMPUMAG'97 chairman.

Albert Foggia was born in Tunis (Tunisia) in April 12, 1942. He obtained his Engineer's and Doctor's degrees in 1964 and 1966 respectively from the *Institut National Polytechnique de Grenoble* (INPG). After graduation he went to Canada where he was assistant Professor at the Moucton University until 1969, and at *Ecole Polytechnique de Montreal* from 1969 to 1971. He came in 1971 to the *Ecole centrale de Lyon* where he was Professor until 1986. Since 1986 he has been Professor at INPG where he teachs electrical machine theory. His main research fields of interest deal with machine modelling, mechanical vibration of electrical machines and design of classical and non conventional machines.